Macromolecules
ARTICLE

Macromolecules **2010**, *43*, 2713–2720 **2713**
DOI: 10.1021/ma902709p

Alternating Amphiphilic Multiblock Copolymers: Controlled Synthesis via RAFT Polymerization and Aqueous Solution Characterization

Natalie A. Hadjiantoniou,[†] Theodora Krasia-Christoforou,[‡] Elena Loizou,[†] Lionel Porcar,[⊥] and Costas S. Patrickios*,[†]

[†]*Department of Chemistry, Faculty of Pure and Applied Sciences, and* [‡]*Department of Mechanical and Manufacturing Engineering, Faculty of Engineering, University of Cyprus, P.O. Box 20537, 1678 Nicosia, Cyprus, and* [⊥]*Institut Laue-Langevin, 6 rue Jules Horowitz, B.P. 156, F-38042 Grenoble, Cedex 9, France*

Received December 9, 2009; Revised Manuscript Received January 31, 2010

ABSTRACT: Four linear amphiphilic multiblock copolymers based on 2-(dimethylamino)ethyl methacrylate (DMAEMA, hydrophilic) and methyl methacrylate (MMA, hydrophobic), bearing from two to five blocks, were synthesized using reversible addition−fragmentation chain transfer polymerization and stepwise monomer additions. The degree of polymerization of each hydrophilic polyDMAEMA block was ∼50, while that of the hydrophobic polyMMA blocks was ca. 20. The stepwise monomer addition procedure secured that each higher multiblock was composed of its immediately lower homologue plus exactly one extra block. The molecular weights (MW) of the synthesized (co)polymers, as measured by gel permeation chromatography (GPC), were close to the theoretically expected. GPC also indicated rather narrow molecular weight distributions which, however, broadened with the number of blocks. The compositions of the copolymers, as determined by proton nuclear magnetic resonance spectroscopy, were also close to the expected values. The cloud points of the copolymers, measured by turbidimetry, were found to increase with the number of blocks. The sizes of the micelles formed by the copolymers in aqueous solution were characterized using dynamic light scattering and small-angle neutron scattering. The determined values of the hydrodynamic radii, the radii of gyration, and the aggregation numbers of the micelles increased slightly with the block number from the triblock to the pentablock copolymer, implying extensive folding of the chains of the tetrablock and the pentablock copolymers in their micelles. The aggregation number of the tetrablock copolymer was approximately one-half that of the diblock copolymer whose unimer MW was one-half that of the tetrablock, suggesting that the micellar cores of these two types of micelles were composed of the same number of hydrophobic units.

Introduction

Multiblock copolymers are linear polymers consisting of several covalently interconnected polymer segments based on two different homopolymers. In addition to the size and composition of the overall multiblock copolymer, it is also necessary to characterize these materials in terms of the size and number of the constituting homopolymer segments (blocks) and their sequence, i.e., typically to clarify whether there is (or not) regular alternation between the two kinds of segments. The nature of the two types of monomer repeating units defines the functional properties of multiblock copolymers, such as their ability to microphase separate in the bulk or in solution and the morphologies obtained.

Multiblock copolymers have been known and studied, but less so than their lower homologues, i.e., diblock and ABA triblock copolymers,[1−3] with which they share many properties and can find similar applications. Because of their higher structural complexity, homogeneous multiblock copolymers are more difficult to synthesize than diblocks and ABA triblocks, and consequently, they are more expensive. Thus, multiblocks are used only when they provide a clear advantage over their lower homologues. A characteristic example is their use as homopolymer blend compatibilizers, where two thermodynamically incompatible homopolymer microphases are "stitched" together via an interfacially active agent, a block copolymer in this case. The good binding between the two homopolymer microphases is essential for the efficient stress transfer through the blend which would ensure good mechanical properties for the sample. Fracture toughness measurements by Dadmun and co-workers have shown that ABABA and BABAB pentablock copolymers were better blend compatibilizers than the corresponding diblocks and ABA and BAB triblocks, as the higher multiblocks secured better microphase "stitching" through their multiple interface crossings.[4,5] However, this was true only when the blocks were long enough to ensure sufficient entanglement with and anchoring in the homopolymers.

The synthesis of multiblock copolymers can be performed by three different strategies. The more traditional strategy involves the interconnection of preformed end-functional polymers, usually by polycondensation, which yields products with a rather heterogeneous size distribution ("most probable" distribution in the number of blocks) and, most frequently, without regular block alternation.[6] (However, block alternation can be achieved if ABA triblock copolymers rather than two different homopolymers are used as starting materials.[7]) The second strategy relies on living/controlled polymerizations[8] and multiple (sequential or stepwise) additions of monomers.[9] These polymer synthesis methods are relatively demanding in that they require specialized initiators, very pure monomers and solvents, and inert reaction conditions (oxygen- and moisture-free), but they readily secure relatively good size and composition homogeneities, a

*To whom correspondence should be addressed. E-mail: costasp@ucy.ac.cy.

Published on Web 02/12/2010

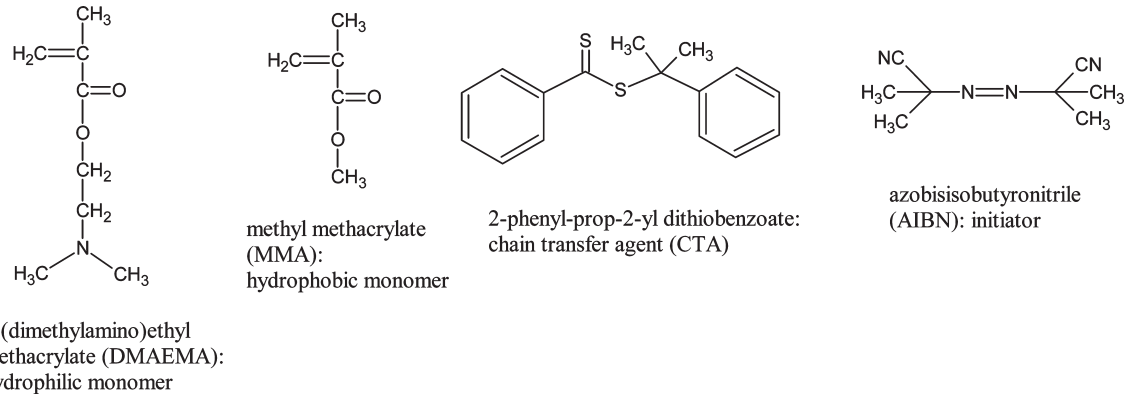

Figure 1. Chemical structures and names of the main reagents used for the polymer synthesis.

predetermined number of blocks (equal to the number of additions of monomer, in the cases when a monofunctional initiator is used), and regular block alternation. The third strategy is a very new one and is based again on controlled polymerizations. However, rather than using simple mono- or bifunctional initiators, it employs multifunctional ones, typically bearing 10 or more initiating sites.[10] Thus, in principle, this new strategy can effect the preparation of a well-defined eicosablock (20-block) copolymer with alternating block types in just two monomer addition steps. However, because of existing limitations of the method, the products obtained exhibit broad size distributions (arising from the size polydispersity of the oligomeric initiator) and a number of blocks lower than that dictated by the number of initiating groups in the multifunctional initiator (arising from active site–typically a radical–migration during the polymerization).

We have recently embarked on a research involving water-compatible, amphiphilic multiblock copolymers, with focus on their self-assembly in aqueous media. Literature on water-soluble multiblock copolymers is very limited; even more limited is literature on the aqueous solution micellization of such systems. To secure the homogeneity of our multiblock copolymers, we employed the second strategy for their preparation, using sequential group transfer polymerization (GTP).[11] The first two systems we explored were conetworks based on end-linked amphiphilic multiblock copolymers.[12,13] All conetworks were characterized in terms of their aqueous degrees of swelling (DSs). In the first system, the block number increased with the overall copolymer size and at constant block sizes; under these conditions, the hydrophile content fluctuated with the number of blocks. The DSs of this system monotonically increased with the hydrophile content, without presenting any systematic dependence on the number of blocks.[12] In contrast, the DSs of the second system consistently increased with the number of blocks;[13] in this system the block number increased at constant overall molecular weight and composition of the multiblock copolymers, achieved by the reduction of the block sizes with block number. The reduction of the length of the hydrophobic blocks provided a weaker driving force for microphase separation, allowing more extensive swelling in the conetworks with a greater number of (shorter) blocks.

The third system was the most interesting one. It was based on linear multiblock copolymers where the block number increased with the overall molecular weight and at constant block sizes.[14] Scattering experiments on aqueous solutions of the multiblock copolymers indicated that the triblock, the tetrablock, and the pentablock copolymers formed micelles but with very small aggregation numbers, typically 3. We attributed the low aggregation numbers to the short lengths of the hydrophilic blocks with degrees of polymerization (DPs) of 20, which conferred stiffness to these blocks and imposed an increased energetic cost for loop formation. To check this hypothesis, in the present study, we prepare bigger multiblock copolymers, whose hydrophilic blocks are 2.5 times longer (DP = 50) compared to the previous system. However, this required the use of a different synthetic method, reversible addition–fragmentation chain transfer (RAFT) polymerization[15] instead of GTP, which allows the preparation of larger polymers. These larger multiblock copolymers are thoroughly characterized in terms of their size and composition, and their aqueous micellization properties are probed using dynamic light (DLS) and small-angle neutron scattering (SANS).

Experimental Section

Materials. The monomers 2-(dimethylamino)ethyl methacrylate (DMAEMA, 98%, hydrophilic) and methyl methacrylate (MMA, 99%, hydrophobic), basic alumina, calcium hydride (CaH_2, 90–95%), and 2,2-diphenyl-1-picrylhydrazyl hydrate (DPPH, 95%) were all purchased from Aldrich, Germany. The initiator 2-azobis(isobutylnitrile) (AIBN) was purified by recrystallization from ethanol and stored in the freezer. Deuterated chloroform ($CDCl_3$) was purchased from Merck, Germany. Benzene and tetrahydrofuran (THF, 99.8%, HPLC) were purchased from Labscan, Ireland.

Methods. Figure 1 shows the chemical structures and names of the monomers, the initiator, and the chain transfer agent (CTA) used for the polymer synthesis. The CTA was synthesized according to the literature.[16] DMAEMA and MMA were passed through basic alumina columns to remove the inhibitor and all other acidic impurities. The monomers were subsequently stirred overnight over CaH_2 to neutralize any traces of water. This was done in the presence of the free radical inhibitor DPPH. The monomers were finally freshly distilled prior to use. The solvent was also stirred overnight over CaH_2 and was freshly distilled prior to use. The CTA was stored in the fridge at 4 °C and was dried overnight under vacuum before use.

Polymer Synthesis. The polymers were synthesized using RAFT polymerization. In total, five polymers were synthesized: one of them was the homopolymer of the hydrophilic DMAEMA, and the others were copolymers of DMAEMA with the hydrophobic MMA, bearing from two up to five blocks. For the synthesis of the homopolymer, a single-neck round-bottom flask was charged with 2.5 mL of benzene (solvent), 7 mL of the DMAEMA monomer (6.53 g, 42 mmol), 70 mg of AIBN initiator (0.426 mmol), and 0.220 g of chain transfer agent 2-phenylprop-2-yl dithiobenzoate (0.808 mmol). The solution was degassed by three consecutive freeze–pump–thaw cycles. Following that, the reaction mixture was heated in an oil bath at 63 °C under stirring for 15 h. Subsequently, the synthesized homopolymer of DMAEMA was precipitated in *n*-hexane and was vacuum-dried at room temperature for 2 days and analyzed by GPC (monomer conversion = 87%; polymer number-average MW = M_n = 8480 g mol^{-1} compared with 7031 g mol^{-1},

which was theoretically expected; polydispersity index = PDI = M_w/M_n = 1.26; M_w is the weight-average MW). For the synthesis of the copolymers, a similar procedure was followed, and instead of dissolving CTA in the polymerization flask, a calculated amount of polymer in which CTA was incorporated (macroCTA) was dissolved. In particular, for the synthesis of the diblock copolymer, 31 mg of AIBN (0.189 mmol) and 5.0 g of the synthesized homopolymer of DMAEMA (0.590 mmol) were dissolved in 6.1 mL of benzene. Then, 1.2 mL of MMA (1.12 g, 11 mmol) was added, and the solution was degassed by three consecutive freeze−pump−thaw cycles. Subsequently, the reaction mixture was heated again in an oil bath at 63 °C under stirring for 19.5 h, and the synthesized diblock copolymer was then precipitated again in *n*-hexane and was vacuum-dried at room temperature for 2 days and analyzed by GPC (monomer conversion = 96%; M_n = 10 600 g mol^{-1} compared with 10 234 g mol^{-1}, which was theoretically expected; PDI = 1.32) and ^{1}H NMR spectroscopy (found 25.2 mol % MMA compared with 25.7 mol %, which was theoretically expected). The synthesis of the triblock copolymer was similarly accomplished by dissolving 89 mg of AIBN (0.0542 mmol) and 3.0 g of the diblock copolymer (0.283 mmol) (which was also dried overnight under vacuum) in 3.8 mL of benzene. Then, 2.6 mL of DMAEMA (2.42 g, 15 mmol) was added, and three consecutive freeze−pump−thaw cycles were followed for degassing the solution. Afterward, the mixture was heated again at 63 °C under stirring for 19 h. After cooling the reaction mixture, the synthesized triblock copolymer was also precipitated in *n*-hexane and vacuum-dried at room temperature for 2 days and analyzed by GPC (monomer conversion = 93%; M_n = 16 400 g mol^{-1} compared with 17 173 g mol^{-1}, which was theoretically expected; PDI = 1.48) and ^{1}H NMR spectroscopy (found 15.4 mol % MMA compared with 15.8 mol %, which was theoretically expected). The tetrablock copolymer was then synthesized by adding 0.35 mL of MMA (0.328 g, 3 mmol) in a mixture of 8.9 mg of AIBN (0.0542 mmol) and 3.0 g of the synthesized triblock copolymer (0.183 mmol) dissolved in 3.8 mL of benzene. Then, the reaction mixture was degassed by the three consecutive freeze−pump−thaw cycles, and after that it was heated in an oil bath at 63 °C under stirring for 19.5 h. As in the previous copolymer synthesis, the synthesized tetrablock copolymer was precipitated in *n*-hexane and vacuum-dried at room temperature for 2 days and analyzed by GPC (monomer conversion = 99%; M_n = 17 300 g mol^{-1} compared with 18 803 g mol^{-1}, which was theoretically expected; PDI = 1.58) and ^{1}H NMR spectroscopy (found 26.0 mol % MMA compared with 26.2 mol %, which was theoretically expected). Finally, the pentablock copolymer was synthesized by adding 0.8 mL of DMAEMA (0.746 g, 5 mmol) in a mixture of 5.5 mg of AIBN (0.0335 mmol) and 2.0 g of the synthesized tetrablock copolymer (0.116 mmol), which was also dried overnight under vacuum, all dissolved in 2.9 mL of benzene. The whole mixture was then degassed by three consecutive freeze−pump−thaw cycles, and afterward it was heated in an oil bath at 63 °C under stirring for 18.5 h. Finally, the synthesized pentablock copolymer was precipitated in *n*-hexane and vacuum-dried at room temperature for 2 days and was analyzed by GPC (monomer conversion = 95%; polymer M_n = 23 100 g mol^{-1} compared with 25 065 g mol^{-1}, which was theoretically expected; PDI = 1.83) and ^{1}H NMR spectroscopy (found 19.9 mol % MMA compared with 20.0 mol %, which was theoretically expected).

Polymer Characterization. *GPC and ^{1}H NMR.* All the synthesized polymers were characterized in terms of their molecular weight (MW) and composition using GPC and ^{1}H NMR spectroscopy, respectively. GPC was performed on a Polymer Laboratories system equipped with a Waters 515 isocratic pump, an ERC-7515A Polymer Laboratories refractive index (RI) detector, and a PL Mixed "D" column. The eluent was THF, pumped at 1 mL min^{-1}. The calibration of the instrument was performed using polyMMA (PMMA) MW standards also supplied by Polymer Laboratories. A 300 MHz Avance Bruker spectrometer equipped with an Ultrashield magnet was used for recording the ^{1}H NMR spectra of the polymers in $CDCl_3$. The copolymer composition was calculated from the ratio of the normalized peak area due to the two oxymethylene protons of DMAEMA divided by that due to the three methoxy protons of MMA, appearing at 4.0 and 3.6 ppm, respectively.

Aqueous Solution Characterization. *Hydrogen Ion Titration.* 5 g of 1% w/w (co)polymer solutions was titrated using a 0.5 M NaOH standard solution in the pH range from 2 to 12. The pH of the solution was measured using a Corning PS30 portable pH meter. The effective p*K*s of the DMAEMA units were calculated as the corresponding pHs at 50% ionization. The pH at which any polymer precipitation occurred during the titration was also noted.

Turbidimetry. The cloud points of 1% w/w (co)polymer solutions in three aqueous solvents were determined using turbidimetry. The first solvent was pure water, which, however, could not dissolve the tetrablock and the pentablock copolymers. The two other solvents dissolved all multiblock copolymers, and these were a 75:25 v/v water:THF mixture and a 50 mM Tris buffer solution at pH 8. For the preparation of the (co)polymer solutions in the water−THF solvent mixture, the copolymers were first dissolved in THF, and the resulting solution was diluted in the appropriate volume of water. A Lambda 10 UV−vis spectrophotometer from Perkin-Elmer was used for the turbidity measurements. The polymer solutions were placed in a quartz cuvette with a path length of 10 mm and kept under stirring during the measurement. A small temperature sensor was immersed in the heated solution. The optical density at 500 nm and the temperature were measured using the TempLab (version 1.56) software. The cloud point was determined as the temperature at which the optical density presented the first abrupt increase.

Dynamic Light Scattering. 1% w/w aqueous solutions of the (co)polymers in the presence of 1 M NaCl at pH ∼ 3 were characterized in terms of their hydrodynamic diameter, using dynamic light scattering (DLS). A 90Plus Brookhaven dynamic light scattering spectrophotometer, equipped with a BI9000 correlator and a 30 mW red diode laser operating at 673 nm, was used for the scattering experiments which were performed at room temperature, whereas the scattering intensity at 90° was recorded. The data were processed using multimodal size distribution (MSD) analysis based on non-negatively constrained least-squares (NNCLS). Prior to the light scattering measurements, the polymer solutions were filtered five times through 0.2 μm PTFE syringe filters and were left at rest for ∼1 h so that any air bubbles could escape.

Small-Angle Neutron Scattering. All the copolymers of this study were characterized using SANS in D_2O in the presence of 1 M NaCl at pH = 3. The samples were in the fully charged state. SANS measurements were performed on the 30 m NG3 instrument at the Center for Neutron Research of the National Institute of Standards and Technology (NIST). The incident wavelength λ was 6 Å. Two sample-to-detector distances, 1.00 and 5.00 m, were employed, covering a q-range [$q = (4\pi/\lambda)\sin(\theta/2)$] from 0.01 to 0.55 Å^{-1}. The samples were loaded in quartz cells. The scattering patterns were isotropic, and therefore, the measured counts were circularly averaged. The averaged data were corrected for empty cell and background. The analysis of the SANS data was performed by fitting the model of Gaussian starlike polymers[17] to the whole scattering curve $I(q)$ in order to obtain the radius of gyration, R_g, and the absolute weight-average MW, M_w. For this model, the scattering intensity is given by eq 1:

$$I(q) = c_g \frac{M_w}{N_{AV}\rho^2}(\rho_p - \rho_s)^2 \frac{2}{fx^2}\left[x - (1 - e^{-x}) + \frac{f-1}{2}(1 - e^{-x})^2\right] + I_{inc}$$

$$x = \frac{f}{3f-2} q^2 {R_g}^2 \qquad (1)$$

Figure 2. Structures of the multiblock (co)polymers synthesized. The hydrophilic DMAEMA units are colored in light blue, whereas the hydrophobic MMA units are painted dark red. D and M are further abbreviations for DMAEMA and MMA, respectively.

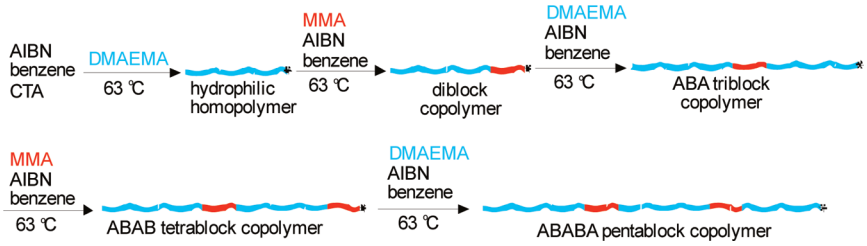

Figure 3. Synthetic procedure followed for the synthesis of the multiblock (co)polymers of this study. The color coding is the same as that in Figure 2.

Table 1. Monomer Conversions, Molecular Weights, and Compositions of All the (Co)polymers of This Study

				GPC results			% mol MMA	
no.	polymer structure[a]	monomer conversion (%)	theor MW[b]	M_n	M_p	M_w/M_n	theory[b]	^{1}H NMR
1	D_{52}	87	7031	8480	10900	1.26	0	0
2	D_{52}-*b*-M_{18}	96	10234	10600	13700	1.32	25.7	25.2
3	D_{52}-*b*-M_{18}-*b*-D_{44}	93	17173	16400	26200	1.48	15.8	15.4
4	D_{52}-*b*-M_{18}-*b*-D_{44}-*b*-M_{16}	99	18803	17300	29400	1.58	26.2	26.0
5	D_{52}-*b*-M_{18}-*b*-D_{44}-*b*-M_{16}-*b*-D_{40}	95	25065	23100	36400	1.83	20.0	19.9

[a] D: DMAEMA, M: MMA; the DPs for each block were calculated from the compositions determined by ^{1}H NMR spectroscopy and the M_n of the homopolymer, determined by GPC. [b] The monomer conversion and the MW of the CTA fragment were also included in the calculation.

Here c_g is the mass concentration of the copolymer, N_{AV} is the Avogadro number, ρ is the density of the polymer taken equal to 1.19 g mL^{-1}, ρ_p and ρ_s are the scattering length densities of the copolymer and the solvent, respectively, and f is the aggregation number of the micelle, which is given by the ratio M_w(micelle)/M_n(chain). Finally, I_{inc} is the constant incoherent background scattering that mostly arises from the H atoms present in the samples. For ρ_s, we employed the value of deuterium oxide of 6.37×10^{10} cm^{-2}. The ρ_p values were polymer-specific and were calculated from the copolymer composition and using homopolymer ρ_p values of 8.23×10^9 and 10.5×10^9 cm^{-2} for polyDMAEMA and polyMMA, respectively. The thus-calculated copolymer ρ_p values ranged between 8.46×10^9 and 8.63×10^9 cm^{-2}.

Results and Discussion

Polymerization Methodology. The structures of the synthesized (co)polymers are schematically represented in Figure 2, while the synthetic procedure followed for their synthesis is illustrated in Figure 3. The synthesis of the (co)polymers was performed via stepwise additions of monomers. The first step resulted in the preparation of the $DMAEMA_{52}$ homopolymer, having one active end (indicated by an asterisk in Figure 3). The second step led to the synthesis of the $DMAEMA_{52}$-*b*-MMA_{18} diblock copolymer, again with one active end. Further stepwise monomer additions provided the other multiblock copolymers with greater numbers of blocks.

Polymer Molecular Weights and Compositions. Table 1 shows the % monomer conversion in the polymerizations, the number-average MWs, M_ns, the peak MWs (MWs at the peak maximum), M_ps, the polydispersity indices, PDIs (M_w/M_n), and the compositions of all the (co)polymers as measured gravimetrically, by GPC, and by ^{1}H NMR spectroscopy, respectively. Figure 4 presents the GPC traces of all the (co)polymers. Table 1 shows that the M_n values of the (co)polymers were close to the theoretically expected MW

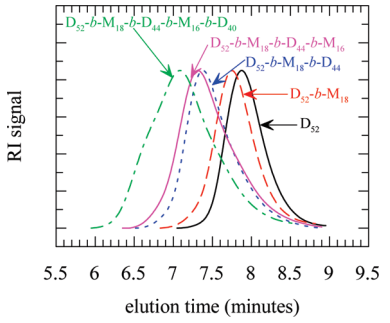

Figure 4. Gel permeation chromatograms of all the (co)polymers of this study prepared by reversible addition−fragmentation chain transfer polymerization. D: 2-(dimethylamino)ethyl methacrylate; M: methyl methacrylate.

values calculated from the monomer/CTA molar ratio in the feed and the monomer conversion, demonstrating the controlled character of RAFT polymerization throughout the synthesis. The molecular weight distributions (MWDs) were relatively narrow but broadened with the number of blocks, with PDIs increasing from 1.26 for the homopolymer to 1.83 for the pentablock copolymer. The MWDs of the homopolymer and the diblock copolymer were relatively narrow, with PDIs of 1.26 and 1.32, and did not present any shoulder or tails in their GPC traces. The triblock and the tetrablock copolymers also exhibited relatively narrow MWDs, with PDIs lower than 1.6, but their GPC traces presented small tails on the low-MW side. The GPC trace of the pentablock copolymer presented a tail on the low-MW side and a small shoulder on the high-MW side, with a relatively high PDI value of 1.83, reflecting the large number of monomer additions.

Our multiblock copolymers bear two kinds of size polydispersity: first, a polydispersity in the size of each block and, second, a polydispersity in the number of blocks. The synthetic technique of stepwise multiple monomer addition

Table 2. Effective p*K*s of the DMAEMA Monomer Repeating Units and pHs of Precipitation of the Multiblock (Co)polymers

no.	polymer structure[a]	pK_{eff}	pH of precipitation
1	D_{52}	7.06	
2	D_{52}-*b*-M_{18}	7.00	9.47
3	D_{52}-*b*-M_{18}-*b*-D_{44}	7.06	
4	D_{52}-*b*-M_{18}-*b*-D_{44}-*b*-M_{16}	7.05	10.28
5	D_{52}-*b*-M_{18}-*b*-D_{44}-*b*-M_{16}-*b*-D_{40}	7.12	10.67

[a] D: DMAEMA, M: MMA.

secures that the multiblock copolymers mainly exhibit the former type of polydispersity. The polydispersity of each block is accumulated and added up in the final multiblock, leading to the higher PDIs of the higher multiblocks. This polydispersity implies the coexistence of multiblock copolymers with the same number of blocks but a distribution in the overall length. The latter type of polydispersity is associated with a distribution in the number of blocks and is probably less extensive than the former type associated with the size distribution of the individual blocks. The block number distribution should be skewed toward the lower number of blocks, based on the synthetic procedure (chain end inactivation) and evidenced from the GPC traces which presented longer tails mainly toward the lower MWs. This means that impurities in a certain sample are lower MW copolymers with a smaller number of blocks.

Monomer conversion was high in all cases, reaching 87% or higher. The copolymer compositions determined from ^{1}H NMR spectroscopy were close to those expected theoretically based on the comonomer feed ratios and the measured monomer conversion. The MMA content in the copolymers was kept relatively low, at 26 mol % or lower, to secure the water solubility of the (co)polymers.

Effective p*K*s and Precipitation pHs. The effective p*K*s of the DMAEMA monomer repeating units and the pHs of precipitation of the (co)polymers as determined using hydrogen ion titration are shown in Table 2. The effective p*K*s of the DMAEMA units in all (co)polymers were determined to be around 7, in agreement with previous investigations on linear polymers containing DMAEMA segments.[18] During titrations, precipitation of the diblock, the tetrablock, and the pentablock copolymers occurred. The homopolymer and the triblock copolymers did not precipitate during titration due to their higher content in the hydrophilic DMAEMA monomer repeating units. Despite its higher DMAEMA content, the pentablock also precipitated most probably due to its higher MW. The pH at which precipitation was observed for the block copolymers is also listed in Table 2.

Polymer Cloud Points. Figure 5 presents the cloud points of the (co)polymers in three aqueous solvents: pure water, a mixture composed of 75% v/v water and 25% v/v THF, and a 50 mM Tris buffer of pH 8. In the same Figure, the mol % DMAEMA composition of the (co)polymers, as determined using ^{1}H NMR spectroscopy, is also plotted against the number of blocks. In all three solvents, the homopolymer of DMAEMA presented the highest cloud point while the diblock copolymer displayed the lowest. The three higher block copolymers exhibited slightly increasing cloud points with the number of blocks. It was expected that the cloud point curve would follow the DMAEMA composition curve which fluctuated with the number of blocks. However, this was not the case, as the cloud points apparently followed the MWs which increased monotonically with the number of blocks. This indicates the dominance of the MW effect on the cloud points over the composition effect. The cloud points of the copolymer solutions in the 75:25 v/v water:THF mixtures

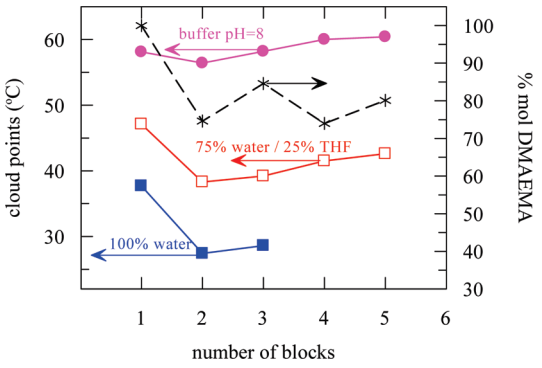

Figure 5. Cloud points and mol % composition in DMAEMA as a function of the number of blocks of all the (co)polymers in three different aqueous solvents.

were ~10 °C higher than those in pure water, while those in the Tris buffer solution at pH 8 were ~30 °C higher than those in pure water.

The present results on the polymer cloud points were important for choosing the most appropriate aqueous environment for the subsequent characterization of the micellar properties of the multiblock copolymers. Pure water was not selected as the appropriate solvent as this could not dissolve all the multiblocks. Although the addition of a small percentage of an organic solvent could result in complete aqueous solubility of the (co)polymers, this was avoided due to the high volatility of organic solvents such as THF. Instead, solubility enhancement was pursued via the full ionization of the DMAEMA units at pH ~ 3. However, to suppress the intense intermolecular Coulombic repulsion in this highly charged system, which might disrupt micellization, the addition of 1 M NaCl was decided.

Micellar Sizes. DLS and SANS were used to determine the micellar sizes of the multiblock copolymers in aqueous solutions. Figure 6 presents the SANS profiles of all the copolymers, which were obtained from 1% w/w solutions in D_2O of pH ~ 3, containing 1 M NaCl. In these dilute dispersions of the copolymers, the scattering intensity depends mainly on the form factor of the particle.[19,20] In the q-regime between 0.01 and 0.55 Å^{-1}, which probes length scales up to several individual micelles, the scattering curves were fitted using the Gaussian starlike polymer model[17] to obtain information about the micelle dimensions. The fits are also shown in Figure 6, and they seem to follow the data well over the entire q-range studied. The R_g and M_w parameters for the micelles obtained from these fits are presented in Table 3, along with the R_h results obtained from DLS. Table 3 also lists the maximum possible micelle radius, R_{max}, calculated from the fully stretched relevant portion of the copolymer chain. For the R_{max} of the tetrablock and the pentablock copolymers, two possible values are given: one for micelles formed by folded copolymer chains and one without folding in the copolymer chains in the corresponding micelle. For the calculation of R_{max}, the M_n values from GPC were used. Finally, Table 3 lists the micellar aggregation numbers, N_{agg}, calculated as the ratio of the M_w of the micelles determined from SANS divided by the M_n of the individual copolymer chains (unimers) determined from GPC.

Figure 7 plots the values of the determined micellar radii R_g, R_h, and R_{max} (for folded copolymer chains for the highest multiblocks) and the aggregation numbers, N_{agg}, against the number of blocks of the multiblock copolymers, whereas Figure 8 illustrates schematic representations of the micellar structures formed on the basis of the determined micellar sizes. All four micellar sizes presented a drop from the

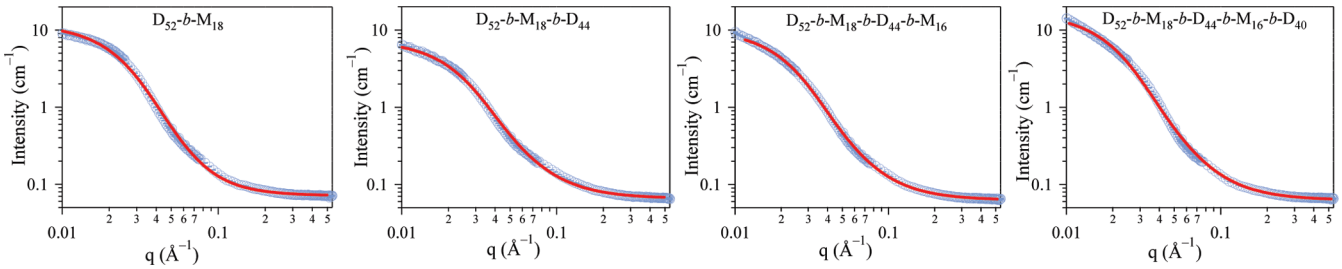

Figure 6. SANS profiles of the four multiblock copolymers in 1% w/w solutions in D_2O of pH ~ 3, containing 1 M NaCl. The dark red continuous lines are fits of the data (light blue symbols) to the Gaussian starlike model.

Table 3. Radii of Gyration, Hydrodynamic Radii, Ratios of the Two Radii, Maximum Radii, Molecular Weights, and Aggregation Numbers of the Micelles Formed by the Multiblock Copolymers in Aqueous Solution

no.	polymer structure[a]	R_g (nm) (SANS)	R_h (nm) (DLS)	R_h/R_g	R_{max} (nm)	$M_{w,micelle}$ (g mol^{-1}) (SANS)	$M_{n,unimer}$ (g mol^{-1}) (GPC)	N_{agg}
1	D_{52}-*b*-M_{18}	8.1	9.8	1.21	17.8	322 000	10 600	31
2	D_{52}-*b*-M_{18}-*b*-D_{44}	8.1	9.2	1.14	15.5	202 000	16 400	12
3	D_{52}-*b*-M_{18}-*b*-D_{44}-*b*-M_{16}	8.5	11.0	1.29	33.0,[b] 23.4[c]	281 000	17 300	16
4	D_{52}-*b*-M_{18}-*b*-D_{44}-*b*-M_{16}-*b*-D_{40}	9.3	11.6	1.25	31.0,[b] 23.4[c]	456 000	23 100	20

[a] D: DMAEMA; M: MMA. [b] Calculated assuming that no chain folding occurs upon micellization. [c] Calculated assuming that the polymer chains in the micelles are folded.

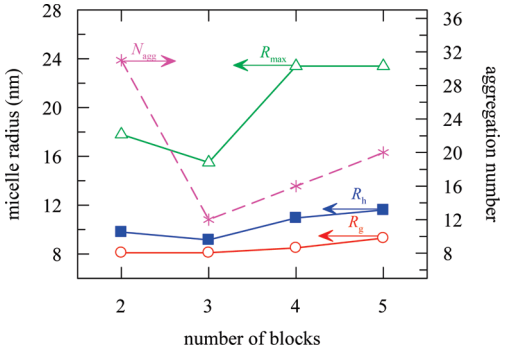

Figure 7. Dependence of the micellar radii and the aggregation number on the number of blocks of the amphiphilic multiblock copolymers in aqueous solution (pH ~ 3, 1 M NaCl).

diblock to the triblock copolymer and then a slight gradual increase from the triblock to the tetrablock and to the pentablock copolymers. All changes in N_{agg} were more pronounced than those in both R_g and R_h. Considering first the micelles formed by the diblock and the triblock, the N_{agg} value for the former was almost 3 times as compared to that of the latter because the composition in MMA hydrophobic units of the former (25 mol %) was almost twice as compared to that of the latter (15 mol %). Another reason for this difference in their N_{agg} values was the greater junction localization requirements for the triblock: the triblock copolymers must accommodate two block junctions at the periphery of the micellar hydrophobic core, whereas the diblock has to accommodate only one. On the other hand, the micellar radii of the triblock were only slightly, if at all, lower than those of the diblock. This was mainly because the chains of the triblock were almost twice as long compared to those of the diblock. In fact, the fully extended length (calculated from the M_n determined by GPC) of the diblock copolymer chain was 18 nm, whereas that of the triblock was 31 nm (Table 3, Figure 8). For the triblock copolymer micelles, their radius should be defined by the extension of half of the copolymer chain (ABA-type micelles), whereas in the case of the diblock copolymer micelles, the radius should be defined by the extension of the whole copolymer chain (AB-type micelles). Considering the limit of fully stretched chains (attained in the hypothetical cases of very large aggregation numbers or very strong electrostatic repulsion), the maximum possible micellar radius (R_{max}) of the diblock copolymer micelles should be 18 nm and that of the triblock 15.5 nm. As the chains were not fully extended within the micelles, the measured radii were about half the above limiting values. The measured R_h value of the triblock copolymer micelles was slightly lower than that of the diblock (9.2 vs 9.8 nm), whereas the same R_g value (8.1 nm) was determined for the micelles of both types of copolymers. The (slightly) greater than expected radii of the triblock copolymer micelles may be attributed to the increased PDI of this copolymer (ca. 1.5) compared to the lower PDI value of the diblocks (ca. 1.3). In particular, the longest of the triblock copolymer chains could lead to an increase in the micellar size as compared to the case when all chains in the triblock copolymer sample were monodisperse. This effect should also be present in the diblocks but to a smaller extent due to the lower PDI in that case.

Regarding the higher multiblocks, their micelles should comprise folded chains (hence, the R_{max} values corresponding only to folded chains are plotted in Figure 7 and indicated in Figure 8) as the micellar radii were not large enough to justify unfolded chain conformations. In fact, the micellar radii of the higher multiblocks were only slightly greater than those of the diblock and the triblock, an observation that excluded the possibility that the higher multiblock chains were overly coiled in their micelles. (There would be no reason for the chains of the higher multiblocks to be more coiled than those of the lower multiblocks in the respective micelles.) The gradual increase of the micellar sizes from the triblock through the pentablock may be attributed to the accompanying increase in the PDIs. In particular, the higher multiblocks, possessing increased PDIs, formed micelles which were larger than those that would be formed in the case of monodisperse systems.

Thus, the higher amphiphilic multiblock copolymers in this study formed micelles with the constituting copolymer chains being folded. This finding is similar to that in our previous work with amphiphilic multiblock copolymers of lower, about half, unimer MWs. However, the N_{agg} values in

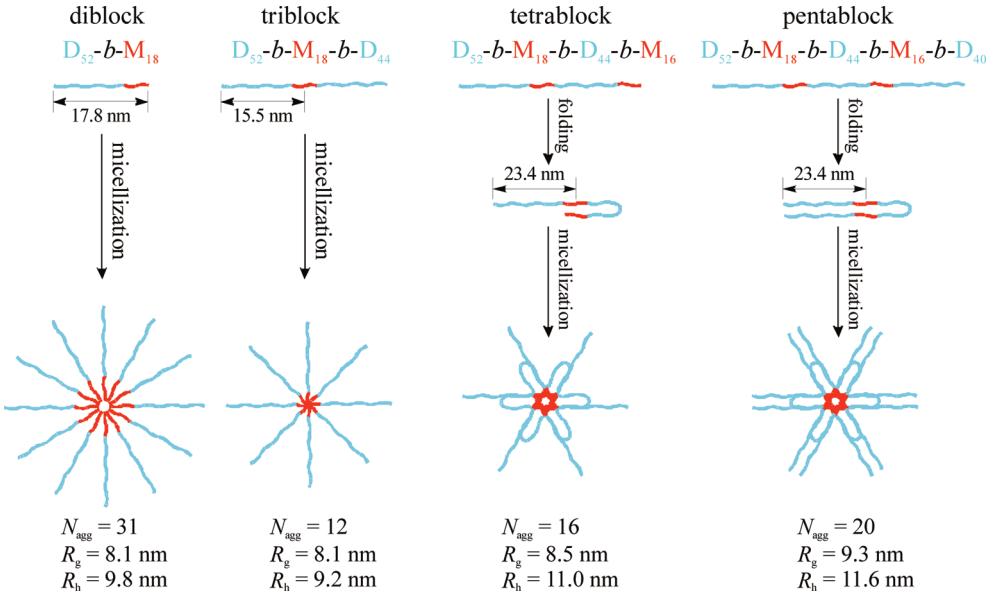

Figure 8. Proposed structures of the micelles formed by the multiblock copolymers in aqueous solution. The preferred micellar structures in the higher multiblocks involve folded copolymer chains. D and M are further abbreviations for DMAEMA and MMA, respectively.

the present system were higher than those in our previous work because of the larger size of the present multiblock copolymer chains. In particular, the longer hydrophobic blocks must have provided a greater driving force for micellization, whereas the longer hydrophilic blocks must have presented a lower overall stiffness and must have been easier to fold. The ease for chain folding with longer (hydrophilic) chains could also have been the reason why the N_{agg} values in the present system were relatively high, increasing with the block number from 12 to 20, whereas the N_{agg} values were constant at 3 in our previous system.[14] An increased block size proved crucial also in the efficiency of multiblock copolymers as blend compatibilizers in the work of Eastman and Dadmun.[4,5] These researchers attributed the beneficial effect of higher block MW on compatibilization efficiency to a better compatibilizer entanglement with and anchoring in the homopolymer phases; however, it is likely that reduced chain stiffness also played an important role.

It is noteworthy that the N_{agg} value for the micelles formed by the tetrablock copolymer (16) was approximately one-half that of the diblock (31). Given that the unimer MW of the tetrablock (17 300 g mol^{-1}) was almost twice as high as that of the diblock (10 600 g mol^{-1}), this implies that the number of hydrophobic MMA monomer repeating units was approximately the same in the two types of micelles. This is in agreement with the predictions of Panagiotopoulos and co-workers,[21] who used Monte Carlo simulations to investigate the micellization behavior of amphiphilic multiblock copolymers. These researchers found that as the number of blocks increases from 2 to 4 to 6, etc., at constant DPs of the solvophilic and the solvophobic blocks and, consequently, the overall size of the unimer doubles, triples, etc., the micellar MW and radius remain constant. To a good approximation this is also the case for the diblock and the tetrablock copolymers of the present study. Note that this was not the case in our previous study with the smaller multiblock copolymers where the micellar MW of the tetrablock was much lower (6 times) than that of the diblock; the micellar radii of that tetrablock were also lower than those of the corresponding diblock by 30% (the R_g) and 40% (the R_h). The deviation in the micellization behavior of the experimental system of the smaller multiblocks from the predictions of the Monte Carlo simulation was probably due to the enhanced stiffness of the rather short chains in the experimental system; the multiblock copolymers in the Monte Carlo simulations were considered infinitely flexible as they were treated as freely jointed polymer chains.[21] The longer chains in the present experimental study were less stiff and, therefore, behaved more closely to those in the simulation.

Finally, the R_h/R_g ratio for all the micelles of this study (Table 3) was around 1.2, close to the value for compact spheres, indicating the compact nature of the micelles formed.

Thus, the results of this study on the micellization of the present multiblock copolymers revealed formation of rather small micelles for the higher multiblocks, indicating polymer chain folding in the formed micelles and confirming the findings of our previous experimental study and a recent simulation. The almost identical size of the micelles formed by the diblock and the tetrablock copolymers of this investigation indicates that the energetic cost for loop formation in these rather long chains is not significant and much lower than that in chains with just one-half of this length.

Conclusions

RAFT polymerization was employed for the synthesis of four amphiphilic multiblock copolymers of DMAEMA and MMA, bearing from two to five blocks. The MWs and the compositions of the (co)polymers were close to the theoretically expected. The cloud points of the copolymers in aqueous solutions were determined and found to increase with the number of blocks and overall MW, exhibiting no strong dependence on copolymer composition which fluctuated with the number of blocks. Finally, the micellar sizes were determined using small-angle neutron scattering and dynamic light scattering. The measurements revealed the formation of rather small micelles, whose radii and aggregation numbers gradually increased from the triblock to the pentablock copolymer. These micellar aggregation numbers were much higher than those in a previous investigation with shorter multiblock copolymers whose stiff hydrophilic blocks were more difficult to fold. The more facile loop formation in the present investigation was also manifested by the ratio of the aggregation

numbers of the micelles formed by the tetrablock divided by that of the diblock copolymers. In particular, the aggregation number in the micelles of the tetrablocks was one-half that of the diblocks, in perfect agreement with the results of a Monte Carlo simulation which treated the chains as infinitely flexible (freely jointed). Future experimental work will involve the preparation and characterization of amphiphilic multiblock copolymers based on different monomer combinations in order to test the validity of the above conclusions for those systems, too.

Acknowledgment. The Cyprus Research Promotion Foundation is thanked for supporting this work in the form of a PENEK 2005 grant (project code: ENISX/0505/019) to NAH. The A. G. Leventis Foundation is also thanked for a generous donation that enabled the purchase of the NMR spectrometer of the University of Cyprus. The National Institute of Standards and Technology (NIST) and U.S. Department of Commerce are acknowledged in providing the neutron research facilities in this work.

References and Notes

(1) Hadjichristidis, N.; Pispas, S.; Floudas, G. A. *Block Copolymers: Synthetic Strategies, Physical Properties, and Applications*; John Wiley & Sons: New York, 2002.
(2) *Amphiphilic Block Copolymers: Self-Assembly and Applications*; Alexandridis, P., Lindman, B., Eds.; Elsevier: Amsterdam, 2000.
(3) Hamley, I. W. *The Physics of Block Copolymers*; Oxford University Press: New York, 1998.
(4) Eastwood, E. A.; Dadmun, M. D. *Macromolecules* **2002**, *35*, 5069–5077.
(5) Eastwood, E.; Viswanathan, S.; O'Brien, C. P.; Kumar, D.; Dadmun, M. D. *Polymer* **2005**, *46*, 3957–3970.
(6) (a) You, Y.-Z.; Zhou, Q.-H.; Manickam, D. S.; Wan, L.; Mao, G.-Z.; Oupický, D. *Macromolecules* **2007**, *40*, 8617–8624. (b) Fang, H.; Zhou, S.; Wu, L. *Appl. Surf. Sci.* **2006**, *253*, 2978–2983. (c) Nagata, M.; Sato, Y. *J. Polym. Sci., Part A: Polym. Chem.* **2005**, *43*, 2426–2439.
(7) (a) Wang, W. J.; Li, T.; Yu, T.; Zhu, F. M. *Macromolecules* **2008**, *41*, 9750–9754. (b) Sasaki, D.; Suzuki, Y.; Hagiwara, T.; Yano, S.; Sawaguchi, T. *Polymer* **2008**, *49*, 4094–4100.
(8) Webster, O. W. *Science* **1991**, *251*, 887–893.
(9) (a) Nagata, Y.; Masuda, J.; Noro, A.; Cho, D.; Takano, A.; Matsushita, Y. *Macromolecules* **2005**, *38*, 10220–10225. (b) Wu, L.; Cochran, E. W.; Lodge, T. P.; Bates, F. S. *Macromolecules* **2004**, *37*, 3360–3368. (c) Spontak, R. J.; Smith, S. D. *J. Polym. Sci., Part B: Polym. Phys.* **2001**, *39*, 947–955. (d) Eastwood, E. A.; Dadmun, M. D. *Macromolecules* **2001**, *34*, 740–747.
(10) (a) Zhou, Y.; Jiang, K.; Song, Q.; Liu, S. *Langmuir* **2007**, *23*, 13076–13084. (b) Zhang, L.; Wang, Q.; Lei, P.; Wang, X.; Wang, C.; Cai, L. *J. Polym. Sci., Part A: Polym. Chem.* **2007**, *45*, 2617–2623. (c) Jia, Z.; Xu, X.; Fu, Q.; Huang, J. *J. Polym. Sci., Part A: Polym. Chem.* **2006**, *44*, 6071–6082. (d) Jia, Z.; Liu, C.; Huang, J. *Polymer* **2006**, *47*, 7615–7620. (e) Pavlović, D.; Linhardt, J. G.; Künzler, J. F.; Shipp, D. A. *J. Polym. Sci., Part A: Polym. Chem.* **2008**, *46*, 7033–7048. (f) Hong, J.; Wang, Q.; Fan, Z. *Macromol. Rapid Commun.* **2006**, *27*, 57–62. (g) Lei, P.; Wang, Q.; Hong, J.; Li, Y. *J. Polym. Sci., Part A: Polym. Chem.* **2006**, *44*, 6600–6606. (h) Wang, Q.; Li, Y.-X.; Hong, J.; Fan., Z.-Q. *Chin. J. Polym. Sci.* **2006**, *24*, 593–597. (i) Bussels, R.; Bergman-Göttgens, C.; Meuldijk, J.; Koning, C. *Macromolecules* **2004**, *37*, 299–9301. (j) Higagi, Y.; Otsuka, H.; Takahara, A. *Polymer* **2003**, *44*, 7095–7101. (k) You, Y.-Z.; Hong, C.-Y.; Pan, C.-Y. *Chem. Commun.* **2002**, 2800–2801. (l) Motokucho, S.; Sudo, A.; Sanda, F.; Endo, T. *Chem. Commun.* **2002**, 1946–1947.
(11) (a) Webster, O. W.; Hertler, W. R.; Sogah, D. Y.; Farnham, W. B.; RajanBabu, T. V. *J. Am. Chem. Soc.* **1983**, *105*, 5706–5708. (b) Sogah, D. Y.; Hertler, W. R.; Webster, O. W.; Cohen, G. M. *Macromolecules* **1987**, *20*, 1473–1488. (c) Dicker, I. B.; Cohen, G. M.; Farnham, W. B.; Hertler, W. R.; Laganis, E. D.; Sogah, D. Y. *Macromolecules* **1990**, *23*, 4034–4041. (d) Webster, O. W. *J. Polym. Sci., Part A: Polym. Chem.* **2000**, *38*, 2855–2860. (e) Webster, O. W. *Adv. Polym. Sci.* **2004**, *167*, 1–34. (f) Raynaud, J.; Ciolino, J.; Baceiredo, A.; Destarac, M.; Bonnette, F.; Kato, T.; Gnanou, Y.; Taton, D. *Angew. Chem., Int. Ed.* **2008**, *47*, 5390–5393. (g) Scholten, M. D.; Hedrick, J. L.; Waymouth, R. M. *Macromolecules* **2008**, *41*, 7399–7404. (h) Raynaud, J.; Gnanou, Y.; Taton, D. *Macromolecules* **2009**, *42*, 5996–6005.
(12) Hadjiantoniou, N. A.; Patrickios, C. S. *Polymer* **2007**, *48*, 7041–7048.
(13) Hadjiantoniou, N. A.; Patrickios, C. S.; Thomann, Y.; Tiller, J. C. *Macromol. Chem. Phys.* **2009**, *210*, 942–950.
(14) Hadjiantoniou, N. A.; Triftaridou, A. I.; Kafouris, D.; Gradzielski, M.; Patrickios, C. S. *Macromolecules* **2009**, *42*, 5492–5498.
(15) (a) Chiefari, J.; Chong, Y. K.; Ercole, F.; Krstina, J.; Jeffery, J.; Le, T. P. T.; Mayadunne, R. T. A.; Meijs, G. F.; Moad, C. L.; Moad, G.; Rizzardo, E.; Thang, S. H. *Macromolecules* **1998**, *31*, 5559–5562. (b) Moad, G.; Rizzardo, E.; Thang, S. H. *Aust. J. Chem.* **2005**, *58*, 379–410. (c) Perrier, S.; Takolpuckdee, P. *J. Polym. Sci., Part A: Polym. Chem.* **2005**, *43*, 5347–5393. (d) Convertine, A. J.; Lokitz, B. S.; Lowe, A. B.; Scales, C. W.; Myrick, L. J.; McCormick, C. L. *Macromol. Rapid Commun.* **2005**, *26*, 791–795. (e) Moad, G.; Rizzardo, E.; Thang, S. H. *Aust. J. Chem.* **2006**, *59*, 669–692. (f) Barner-Kowollik, C.; Buback, M.; Charleux, B.; Coote, M. L.; Drache, M.; Fukuda, T.; Goto, A.; Klumperman, B.; Lowe, A. B.; Mcleary, J. B.; Moad, G.; Monteiro, M. J.; Sanderson, R. D.; Tonge, M. P.; Vana, P. *J. Polym. Sci., Part A: Polym. Chem.* **2006**, *44*, 5809–5831. (g) Favier, A.; Charreyre, M.-T. *Macromol. Rapid Commun.* **2006**, *27*, 653–692. (h) Lowe, A. B.; McCormick, C. L. *Prog. Polym. Sci.* **2007**, *32*, 283–351.
(16) Becke, F.; Hagen, Ger. H. 1274121, **1968**; *Chem. Abstr. 70*, 3573v.
(17) Benoit, H. *J. Polym. Sci.* **1953**, *11*, 507–510.
(18) Simmons, M. R.; Patrickios, C. S. *Macromolecules* **1998**, *31*, 9075–9077.
(19) Yang, L.; Alexandridis, P. *Langmuir* **2000**, *16*, 4819–4829.
(20) Yang, L.; Alexandridis, P. *Macromolecules* **2000**, *33*, 3382–3391.
(21) Gindy, M. E.; Prud'homme, R. K.; Panagiotopoulos, A. Z. *J. Chem. Phys.* **2008**, *128*, 164906.